Scientific Research and Essays Vol. 5 (9), pp. 911-916, 4 May, 2010
Available online at http://www.academicjournals.org/SRE
ISSN 1992-2248 © 2010 Academic Journals

*Full Length Research Paper*

# Deformation of Eastern Turkey from seismic and geodetic strain rates

**Asli Dogru**

Bogazici University, Kandilli Observatory and Earthquake Research Institute, Geodesy Department, 34680 Cengelkoy, Istanbul, Turkey. E-mail: asli.dogru@boun.edu.tr. Tel: +90 216 516 33 77. Fax: +90 216 332 02 41.

Accepted 6 April, 2010

**Crustal deformation is the study of active geophysical processes that occur within the earth's lithosphere. Geodesy provides facilities to investigate the earth's crust movements and shares these data with the other disciplines. The various sources of geodetic data can be used to observe crustal deformation. Especially, GPS has gained wider acceptance worldwide for monitoring crustal dynamics for earthquake studies. GPS velocities help to improve the estimation of long-term strain rate tensor field. Seismic strain rates are also essential for determining seismic hazard of a region. Current studies show agreement between seismic strain rates inferred from earthquakes and regional tectonic strain patterns. In this study, a strain rate model was presented for the Eastern Turkey based on GPS velocities and earthquake focal mechanisms. The dense data coverage in this region allows a comparison of the seismic strain rate field with tectonic strain rate field observed geodetically. The principal strain rates were derived from the 16 GPS velocities (2003 - 2006) relative to Eurasia, which are in the range of 16 - 24 mm/year, and moment tensors of moderate-sized earthquakes with 30 years time span. The results are consistent with the current studies and strain rates confirm the active state of the secondary faults in the region.**

**Key words**: Crustal deformation, GPS, seismicity, NAFZ, EAFZ, focal mechanisms.

## INTRODUCTION

Anatolian Plate, which is squeezed by the movement of Eurasia, Africa and Arabian plates, has major active fault zones; North Anatolian Fault Zone (NAFZ) and East Anatolian Fault Zone (EAFZ). This study focuses on the Eastern Turkey (Figure 1). The active tectonics of Eastern Turkey is mainly dominated by the right-lateral NAFZ (Sengor, 1979; Dewey and Sengor, 1979; McClusky et al., 2000), running from Karliova country in the NE to Istanbul in the NW and left-lateral EAFZ (McKenzie, 1972; Jackson and McKenzie, 1988; Aksoy et al., 2007), running from Karliova country in the NE to Hatay in the SW. In this study, GPS observations and earthquake moment tensors are combined to obtain a kinematic model for the region of interest.

Geodetic and seismic strain rate fields are obtained using the method developed by Haines and Holt (1993), which allows the estimation of strain rates by integrating seismic and geodetic data. The GPS measurements for the period of 2003 - 2006 come from Ozener et al. (2010). In order to define a seismic strain rate field, moment tensors from Global CMT Catalog are used. Global CMT catalog has moment tensors for earthquakes with M > 5 since 1976. Since the lithosperic deformation is studied, shallow events (with a depth less than 30 km) are used (Figure 2).

As shown in Figure 2, fault plane solutions imply that the faulting type in the region is strike-slip faulting. Furthermore, some of the earthquakes have dip-slip reverse/normal faulting components. Fault plane solutions of 2004 Sivrice-Elazig earthquakes indicate that the region is mainly characterized by left-lateral strike-slip faulting. And the earthquakes are occurring along the strike-slip faults with generally compression component and partially normal component.

Focal mechanism solutions of 2005 Karliova-Bingol earthquakes show right-lateral strike-slip faulting and some of the earthquakes have dip-slip reverse faulting character. In this study, GPS data provide velocity gradient tensor field while mechanisms of moderate-sized earthquakes are used to help for constrain on the


**Figure 1.** Tectonic setting of Turkey and the study area.

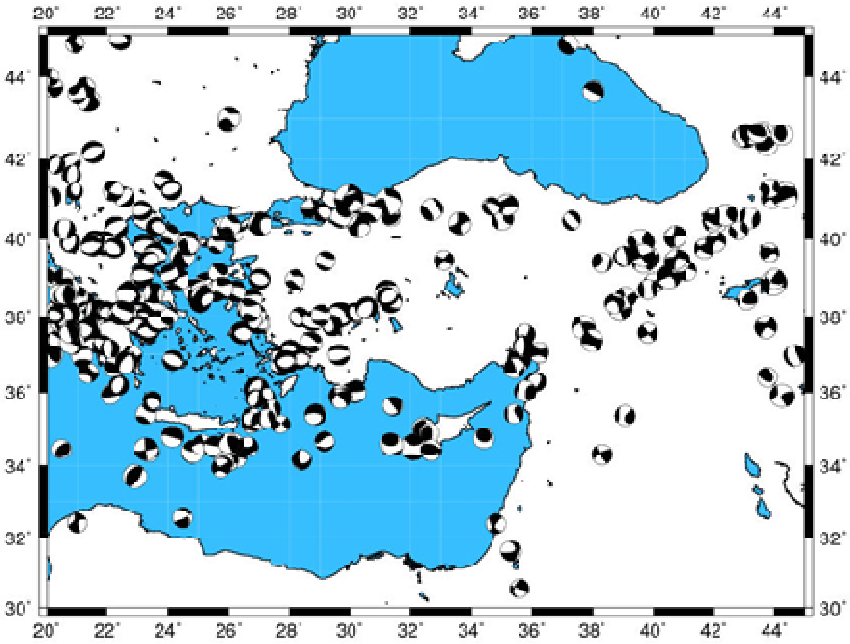


**Figure 2.** Focal mechanisms (beach balls) with M > 5.0.

direction and style of strain in the region.

## METHOD USED FOR ESTIMATING STRAIN RATE FIELD

According to Haines and Holt (1993), the horizontal velocity field u(r) for the spherical earth expressed as

$$u(\hat{x}) = rW(\hat{x}) \times \hat{x} \quad (1)$$

Where, r is the radius of the Earth and $\hat{x}$ is the position vector on the Earth's surface. This method allows the combination and comparison of different data types. It determines $W(\hat{x})$ at the

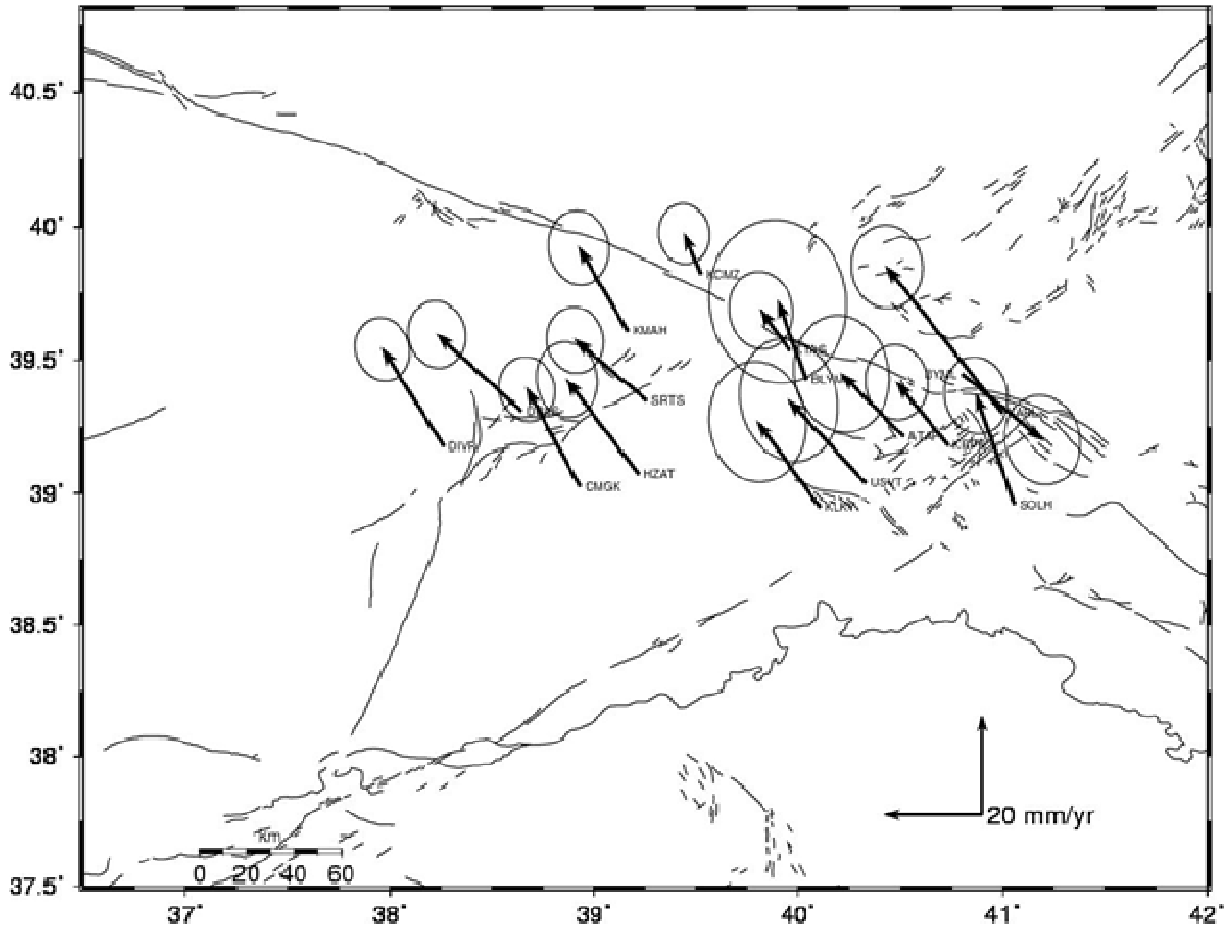


**Figure 3.** Horizontal velocity field of the region in a Eurasia-fixed reference frame (ellipses are at 95% confidence level). Black lines represent regional faults (Saroglu et al., 1992).

nodes of a rectangular grid using bi-cubic spline interpolation. These values are obtained from least-squares inversion between observed and predicted values of strain rate and velocity. Depending on the data distribution on the study region, smoothing between neighboring grid cells is required. No smoothing takes no account of how the strain rates are distributed in neighboring rectangles, in which the strain rates may be significantly higher or lower. In the case of seismic data inversion, strain rates are estimated from Kostrov summation (1974):

$$\dot{\bar{\varepsilon}}_{ij} = \frac{1}{2\mu VT}\sum M_0 m_{ij} \quad (2)$$

Where, $\mu$ is the shear modulus, V is the cell volume (the grid area times the seismogenic thickness), T is the time period of the earthquake record, $M_0$ is the scalar seismic moment, and $m_{ij}$ is the unit moment tensor. Shear modulus is taken as $3.5\times10^{10}\,Nm^{-2}$, and seismogenic thickness is 30 km. These chosen values affect the magnitude but not the style of the estimated strain rates.

Geodetic velocities are the changes in location of campaign-based GPS sites. These data are used as input data into a strain rate model which then calculated strain on an array over the study region. A spline interpolation technique is applied in which model velocities are fitted to observed GPS velocities, and those are then interpolated to derive a continuous velocity gradient tensor field which implicitly defines the strain rate tensor everywhere (Figure 3) In this study, the model grid is continuous in longitudinal and latitudinal directions and covers the study area. The model is calculated on a regular grid. Each grid area is 0.5° x 0.5° in dimension whether an area is considered to be deforming or not is based primarily on seismicity occurrence (Ambraseys and Finkel, 1995; The Global CMT Catalog, 2009; KOERI Earthquake Catalog, 2009).

## RESULTS AND CONCLUSION

In order to define the best estimate of the seismic strain rate field, the events up to M = 6.5 are used. It is seen that the strain rate field is dominated by larger events. Moreover, the results of the seismic strain rates depend on the seismogenic thickness. Different values may result in different moment rates. In case of inversion of GPS data, observed strain rates are not used. GPS velocities

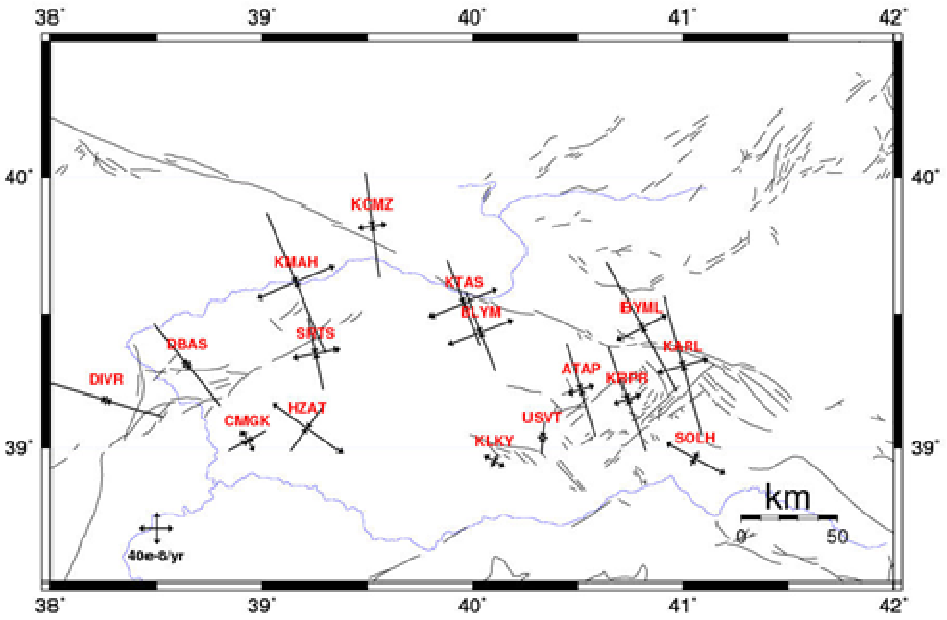


**Figure 4.** Strain rates obtained from fitting GPS velocities plotted in Figure 3 (inside and outside arrows indicate extension and compression, respectively). Black lines represent regional faults (Saroglu et al., 1992).

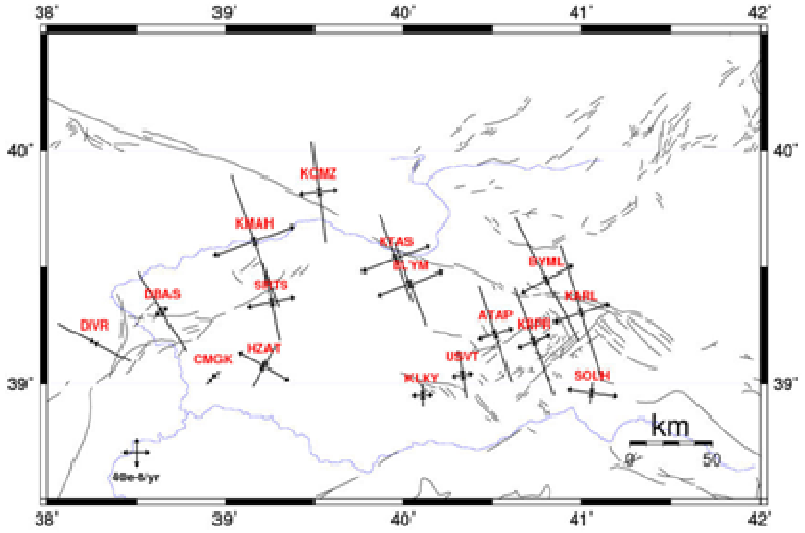


**Figure 5.** Strain rates obtained from fitting GPS velocities with constraints from seismicity (inside and outside arrows indicate extension and compression, respectively). Black lines represent regional faults (Saroglu et al., 1992).

are matched while no priori constraints are placed on the style and direction of the model strain rate field. Importantly, the GPS data coverage in the region affects to define a reliable long-term strain rate field (Kreemer, 2000). The geodetic deformation field is dominated by right-lateral strike-slip deformation along the NAFZ. The geodetic strain rate field (Figure 4) is found much smoother, which reflects the differing characters of long-term tectonic and short-term seismic strain rates.

In the inversion of GPS data with constraints from seismicity, only the direction and relative magnitude of the principal axis of strain rate constrained a priori (Figure 5). Whether the strain rates are compressional or extentional, is defined by GPS data. The model strain

**Table 1.** Principal strains computed at GPS sites by the inversion of GPS data with seismic constraints.

| Site | Lon. (deg) | Lat. (deg) | $\varepsilon_1$ ($10^{-8}$ year$^{-1}$) | $\varepsilon_2$ ($10^{-}$ year$^{-1}$) | Azimut (deg) |
|---|---|---|---|---|---|
| KARL | 40.999 | 39.304 | -4.998E+01 | 2.094E+02 | 72.11677 |
| BYML | 40.803 | 39.448 | -4.909E+01 | 2.113E+02 | 62.18207 |
| KRPR | 40.733 | 39.182 | -4.041E+01 | 1.334E+02 | 69.03766 |
| ATAP | 40.515 | 39.215 | -3.566E+01 | 1.315E+02 | 71.31110 |
| USVT | 40.330 | 39.039 | -1.672E+01 | 7.487E+01 | 80.63847 |
| KLKY | 40.105 | 38.949 | -8.294E+00 | 7.734E+01 | 88.28720 |
| BLYM | 40.038 | 39.430 | -3.122E+01 | 2.543E+02 | 69.48848 |
| KTAS | 39.957 | 39.538 | -3.273E+01 | 2.623E+02 | 69.02343 |
| KCMZ | 39.524 | 39.824 | -3.586E+01 | 1.396E+02 | 82.75909 |
| SRTS | 39.258 | 39.350 | -2.743E+01 | 1.767E+02 | 78.29469 |
| HZAT | 39.217 | 39.074 | -1.621E+01 | 2.074E+02 | 118.4613 |
| KMAH | 39.164 | 39.613 | -4.918E+01 | 3.079E+02 | 69.89008 |
| CMGK | 38.931 | 39.026 | -6.424E+00 | 5.177E+00 | 133.6965 |
| DBAS | 38.645 | 39.310 | -3.277E+01 | 5.735E+01 | 58.29931 |
| DIVR | 38.264 | 39.178 | -2.896E+01 | 5.561E+00 | 27.84501 |
| SOLH | 41.057 | 38.959 | -7.661E+00 | 1.824E+02 | 97.90699 |

rate field is obtained from bi-cubic Bessel interpola English tion of GPS velocities with a priori constraints on the style and direction from earthquakes with $M_0 < 1x10^{20}$ Nm are produced in this inversion. As shown in Figures 4 and 5, geodetic strain rate field and seismic strain rate field are very similar in deformation style. East-west compression and North-south extension along NAFZ reflects right-lateral faulting of NAFZ. The results are consistent with the results obtained from Ozener et al. (2010) and strain rates confirm the active state of the secondary faults in the region. Results obtained from the geodetic observations and seismic data are listed in Table 1.

Deformation towards to the West of the Karliova region, which is the conjunction of NAF with EAF, is caused by the strike-slip faulting along NAF and EAF. And the deformation from this intersection area to the east is caused by the thrust faults exist in the region. It is necessary to fulfill more detailed studies in order to gain much more knowledge about the complex kinematics of Eastern Turkey. GPS data plays a critical role in generating strain rates. Therefore, more GPS data coming from an extended and spatially dense GPS network are needed to yield more reliable results. Assessment of strain accumulation in specifically targeted areas can be obtained by using geodetic and seismic data. And this is vital to identify areas of high seismic hazard, which is the most effective way to reduce earthquake losses.

## ACKNOWLEDGEMENTS

Author would like to thank Prof. Dr. Haluk Ozener who conducted the project, supported mainly by TUBITAK-CAYDAG under Grant No. 103Y043 and additionally by Bogazici University-KOERI for the GPS data used in this study.

## REFERENCES

Aksoy E, Inceoz M, Kocyigit A (2007), Lake Hazar basin: A negative flower structure on the east anatolian fault system (EAFS), SE Turkey, Turkish J. Earth Sci. 16: 319-338.

Ambraseys NN, Finkel CF (1995). The Seismicity of Turkey and Adjacent Areas: A Historical Review, 1500-1800. Eren, Istanbul, Turkey.

Dewey JF, Sengor AMC (1979). Aegean and surrounding region: complex multiplate and continuum tectonics in a convergent zone. Geol. Soc. Am. Bull. 90(1): 84-92.

Global CMT Web Page (accessed April 2009). http://www.globalcmt.org

Haines AJ, Holt WE (1993). A procedure to obtain the complete horizontal motions within zones of distributed deformation from the inversion of strain rate data. J. Geophys. Res. 98: 12057-12082.

Jackson J, McKenzie D (1988). The relationship between plate motions and seismic tremors, and the rates of active deformation in the Mediterranean and Middle East. Royal Astron. Soc. Geophys. J. 93: 45-73.

Kostrov VV (1974). Seismic Moment and Energy of Earthquakes, and Seismic Flow of Rocks, Izv Acad. Sci. USSR, Phys. Solid Earth English Trans. 1: 23-44.

KOERI Earthquake Catalog (accessed April 2009). Bogazici University, Kandilli Observatory and Earthquake Research Institute, National Earthquake Monitoring Center, Waveform Data Request System.

Kremeer C, Holt WE, Goes S, Govers R (2000). Active Deformation in Eastern Indonesia and the Philippines from GPS and Seismicity Data. J. Geophys. Res. 105: 663-680.

McClusky S, Balassanian S, Barka A, Demir C, Ergintav S, Georgiev I, Gurkan O, Hamburger M, Hurst K, Kahle H, Kastens K, Kekelidze G, King R, Kotzev V, Lenk O, Mahmoud S, Mishin A, Nadariya M, Ouzounis A, Paradissis D, Peter Y, Prilepin M, Reilinger R, Sanli I, Seeger H, Tealeb A, Toksoz MN, Veis G (2000). Global Positioning System constraints on plate kinematics and dynamics in the eastern Mediterranean and Caucasus. J. Geophys. Res. 105: 5695-5719.

McKenzie D (1972). Active tectonics of the Mediterranean region, Geophys. J. Royal Astron. Soc. 30(2): 109-185.

Ozener H, Arpat E, Ergintav S, Dogru A, Cakmak R, Turgut B, Dogan U

(2010). Kinematics of the eastern part of the North Anatolian Fault Zone. J. Geodynamics 49: 141-150.
Saroglu F, Emre O, Kuscu I (1992). Active Fault Map of Turkey, General Directorate of the Mineral Research and Exploration, Ankara, Turkey.
Sengor AMC (1979). The North Anatolian transform fault: its age, offset and tectonic significance. J. Geol. Soc. 136(3): 269-282.